Macroscopic Supramolecular Assembly to Fabricate 3D Ordered Structures: Towards Potential Tissue Scaffolds with Targeted Modification

Mengjiao Cheng, Yue Wang, Lingling Yu, Haijia Su, Weidong Han, Zaifu Lin, Jianshu Li, Haojie Hao, Chuan Tong, Xiaolei Li, and Feng Shi**

3D ordered structures beyond microscale with targeted modification are catching increasing attention due to its application as tissue scaffolds. Especially scaffolds with necessary growth factors at designated locations are meaningful for induced cell differentiation and tissue formation. However, few fabrication methods can address the challenge of introducing bioactive species to the interior targeted places during the preparation process. Herein, for the first time macroscopic supramolecular assembly is applied to obtain such 3D ordered structures and established a proof-of-concept idea of complex scaffold with targeted modification. Taking strip-like polydimethylsilicon building block as a model system, microscaled multilayered structures have been fabricated with parallel aligned building blocks in each layer. The morphology can be adjusted in a flexible way by tuning the number of layer, the space between two adjacent building blocks, and the position and orientation of each PDMS. The as-prepared 3D structures are demonstrated biocompatible and potential as scaffolds for 3D cell culture. Moreover, bioactive species can be in situ incorporated into designated locations within the 3D structure precisely. In this way, a novel strategy is provided to address the current challenges in fabricating complex 3D tissue scaffolds with localized protein for future induced cell differentiation.

1. Introduction

3D ordered structures at the tens of microns to one millimeter scale are useful for tissue engineering,[1–6] photonic crystals operating at infrared wavelengths,[7] and other applications.[8–10] Notably, this size range fits well with the scale of most cells, which require 3D supporting scaffolds with targeted modification to grow. Especially, there are urgent demands and challenges in fabricating complex 3D tissue scaffolds with in situ localized proteins for directed cell differentiation.[11] Due to the difficulty in fabrication,[12] there are currently only a few methods to prepare these ordered structures. A 3D bioprinting method can be used to reproduce tissue or organs by printing mixtures of living cells, bioactive species, and supporting materials into complex 3D structures.[13] But in this method, it is contradictory to handle the paradox between the increasing resolution of the structure and the accompanied decreasing cell viability. Although the two-photon technique can realize 3D patterning of bioactive proteins with high resolution, specific materials and expensive instrument are necessary.[11] Therefore, a more versatile strategy is needed to obtain 3D ordered structures with targeted modification through biocompatible experimental procedures.

The recent progress of macroscopic supramolecular assembly[14–19] is advantageous in being bottom-up, mild, biocompatible, and instrument-independent that can be used to address the above problems.[20] However, to the best of our knowledge, there are no reports on the preparation of 3D structures with high ordering by macroscopic supramolecular assembly. Here, we have obtained multilayered structures with 3D ordering through combining magnetic field for localization and subsequent macroscopic supramolecular assembly for immobilization, and provided a conceptualized model of 3D scaffolds with targeted modification. By using the strip-like polydimethylsilicon (PDMS) building block as a model system, we fabricated periodically stacked 3D structure through stepwise magnetic-field-induced locomotion and supramolecular assembly of the PDMS strips. The number of stacked layers,

Dr. M. J. Cheng, Y. Wang, L. L. Yu,
Prof. H. J. Su, Prof. F. Shi
State Key Laboratory of Chemical Resource Engineering and Beijing Laboratory of Biomedical Materials
College of Materials Science and Engineering
Beijing University of Chemical Technology
Beijing 100029, P.R. China
E-mail: shi@mail.buct.edu.cn
Prof. W. D. Han, Dr. H. J. Hao,
C. Tong, Dr. X. L. Li
Institute of Basic Medicine Science
College of Life Science
Chinese PLA General Hospital
Beijing 100853, P.R. China
E-mail: hanwdrsw@sina.com
Z. F. Lin, Prof. J. S. Li
College of Polymer Science and Engineering
Sichuan University
Chengdu 610065, P.R. China

DOI: 10.1002/adfm.201503366

the space between adjacent PDMS building blocks and their orientation of the PDMS strips could be controlled and adjusted. Moreover, the as-prepared stacked 3D ordered structures displayed good biocompatibility with three cell types, as indicated by high cell viability and good cell adhesion on the 3D structure. By further introducing a labeled PDMS strip modified with bioactive species into a designated location within the structure, we established a proof-of-concept idea of in situ loading targeted growth factors into 3D tissue scaffolds, which is meaningful for directed differentiation of stem cells.[11]

2. Results and Discussion

2.1. Fabrication of Magnetic-Responsive Strip-Like PDMS Building Blocks

The strip-like PDMS building blocks with a feature size of 150 μm × 150 μm × 2 mm were prepared with the following procedures as illustrated in Scheme S1 (Supporting Information). For precise magnetic field localization,[21–25] we incorporated Fe_3O_4 magnetic nanoparticles into the PDMS building blocks during the fabrication process. First of all, we have synthesized Fe_3O_4 magnetic nanoparticles with an average diameter of 500 nm (Figure S1a,b, Supporting Information) following a reported method.[26] Second, the dried Fe_3O_4 nanoparticles were mixed with dye, PDMS prepolymer and its crosslinking agent through stirring followed by removing of air bubbles. Then a viscous liquid drop of the mixture was sandwiched between two hydrophobic glass slides. The hydrophobic glass slide was obtained by the following procedures: the glass slides were cleaned by a piranha solution (98% H_2SO_4: 30% H_2O_2 = 3:1, v/v), washed with deionized water and dried in nitrogen flow; the cleaned glass slides were then modified with a low-surface-energy coating of 1H, 1H, 2H, 2H-perfluoroalkyltriethoxysilane by chemical vaporized deposition at room temperature for 24 h. The thickness of the thin PDMS film was determined by the spaced cover glass with an average thickness of about 150 μm at the ends of two glass slides. After heated at 65 °C for 1 h to achieve complete crosslinking of PDMS, a sheet of freestanding PDMS film with a thickness of about 150 μm was obtained. Third, this PDMS film was cut into a size of 150 μm × 2 mm × 2 mm and further cut with a freezing microtome instrument to a final dimension of 150 μm × 150 μm × 2 mm. Note that we chose strip-like PDMS building blocks as model systems to demonstrate the feasibility of the proposed macroscopic supramolecular assembly for construction of 3D ordered structure. Based on the versatility of macroscopic supramolecular assembly of rigid building blocks,[18] other biocompatible materials such as polylactic acid, polycaprolactone, and so on are also applicable for the proposed method.

2.2. Surface Modification of PDMS Building Blocks and Supporting Platform

For supramolecular assembly of the as-prepared magnetic-responsive PDMS building blocks, we introduced a typical supramolecular recognition pair of host/guest (cyclodextrin, CD)/(azobenzene, Azo) groups[27] onto the PDMS surfaces through a layer-by-layer (LbL) technique.[28–31] To distinguish building blocks with different surface groups, the CD-modified PDMS strips were pre-dyed red, whereas the Azo-modified strips were pre-dyed green. As shown in **Scheme 1**a, negatively charged poly(acrylic acid) (PAA) grafted with CD (PAA-CD) or Azo (PAA-Azo) (Figure S2, Supporting Information) was alternately deposited with positively charged poly(diallyldimethylammonium chloride) (PDDA) onto PDMS surfaces using LbL assembly. First the cleaned PDMS strips

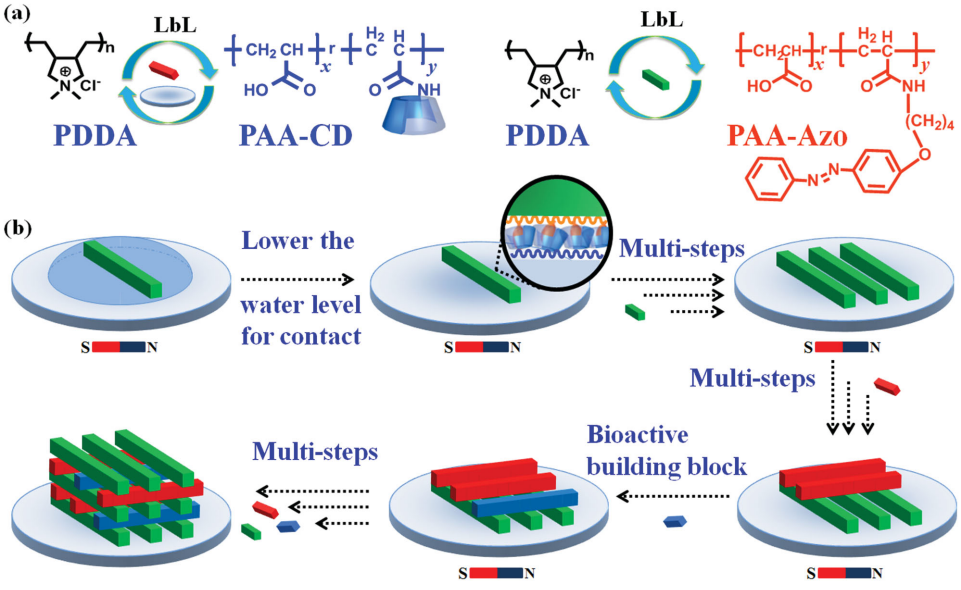

Scheme 1. Illustrations of a) the surface modification by host or guest groups through LbL assembly and b) the stepwise magnetic localization and supramolecular assembly for the fabrication of 3D ordered structure.

were immersed in an aqueous solution of PDDA (1 mg mL^{-1}) for 30 min to reach a saturated adsorption of positively charged PDDA because of physical adsorption. Subsequently, the strips were rinsed with deionized water for three times to remove loosely adsorbed species. Second the PDMS strips with PDDA were transferred to an aqueous solution of PAA-CD (aq., 1 mg mL^{-1}) or PAA-Azo (aq., 1 mg mL^{-1}) for 5 min to result a layer of PAA-CD or PAA-Azo by using the electrostatic interaction between PDDA and ungrafted PAA groups. Similarly, after this step, the strips were washed with deionized water for three times. Third the above two steps were repeated in PDDA for 5 min and in PAA-CD or PAA-Azo for 5 min in a cycled manner. Considering the demands for sufficient host or guest groups on the PDMS surfaces, the final (PDDA/PAA-CD or PDDA/PAA-Azo)$_n$ multilayer (n refers to the number of deposition cycles or bilayers) was optimized at 25 bilayers by checking the stability of the assembled strip on the glass slides in magnetic field at different number of bilayers. The glass slides were LbL assembled with (PDDA/PAA-CD)$_{25}$ as the substrate to support the assembled structures. Special PDMS building blocks with bioactive sites were modified through LbL assembling of alternate immersion in PAH-biotin (poly(allylamine hydrochloride) grafted with biotin, Figure S3, Supporting Information) (aq., 1 mg mL^{-1}, 5 min) and PAA-CD (aq., 1 mg mL^{-1}, 5 min) for 19.5 cycles to give an outmost layer of PAH-biotin. The host and guest groups on the modified PDMS surfaces were expected to interact with each other through host/guest supramolecular recognition when the two PDMS surfaces were drawn to within the molecular interactive distance.

2.3. Fabrication of 3D Ordered Structures Through Macroscopic Supramolecular Assembly

After we obtained the magnetically responsive PDMS building blocks with the host or guest surface groups, we tried to clarify whether we could precisely maneuver the PDMS building blocks to designated locations and further immobilize them through supramolecular interactions, as illustrated in Scheme 1b. Initially, the quartz substrate modified with CD groups was placed at the bottom of a petri dish containing water, whereas Azo-modified PDMS building blocks were dispersed on the water surface. When introducing an external magnetic field by placing a magnet beneath the petri dish, directly below the Azo-modified PDMS building block (strips dyed green), the PDMS building block rapidly aligned along the magnetic induction line in response to the magnetic field. Due to this rapid response, the PDMS building block could then be guided to the targeted location on the quartz substrate. Because the magnetic force is a type of non-contacting long-ranged force, there is sufficient time and space to orientate the building block to the correct position. The water level was then lowered until the PDMS building block contacted the quartz substrate, during which the hydrophilic PDMS building block and the quartz substrate gradually reached the molecular interaction distance. The outermost Azo groups on the PDMS interacted with the CD groups on the substrate through host/guest molecular recognition, leading to the supramolecular assembly of the PDMS building block on the substrate surface. Likewise, more Azo-modified PDMS building blocks could be introduced using the magnetic field and immobilized one after another via supramolecular assembly. Because the previous building blocks were affixed via supramolecular interactions, they remained unaffected by the reapplied magnetic field. This allowed for flexible localization of later building blocks for the construction of 2D and even 3D ordered structures. Otherwise, the unassembled building blocks would align with the later ones in the presence of magnetic field, thus losing control over the intended geometry of the structure.

Although we have assembled one layer of PDMS building blocks parallel to each other, we should explore the feasibility of constructing a periodically stacked 3D ordered structure because the contacting area between the first and second layer would decrease compared with that between the substrate and the first layer. Based on the as-prepared first layer of Azo-PDMS, the CD-modified PDMS building blocks (strip dyed red) were used to construct the second layer through the host/guest recognition with the Azo-modified PDMS on the first layer; following this concept, a third layer could be achieved using the Azo-modified PDMS building blocks. Using the above step-by-step magnetic localization and supramolecular assembly, periodically stacked 3D ordered structures were obtained (**Figure 1**b–d).

2.4. 3D Profile of the 3D Ordered Structures Compose of PDMS Building Blocks

After we obtained 3D ordered PDMS structures, we characterized their morphology with a 3D profiler. From the sectional and top views in Figure 1a and **Figure 2**, respectively, we can observe that the average length, width, and height of all three PDMS building blocks were approximately 2.0 ± 0.1 mm, 138 ± 7 μm, and 154 ± 10 μm, respectively, which was in agreement with the designed feature size. The horizontal spacing between blocks was controlled during the magnetic localization to be approximately 381 ± 8 μm, indicating that the accuracy of magnetic localization could be controlled on the micron scale. Notably, the direction and spacing of the targeted PDMS building blocks could be frequently adjusted via magnetic localization before the building block contact the substrate. Therefore, the localization accuracy could be further improved to the sub-micron level with precise magnetic manipulation system according to previous research by the Whitesides and co-workers.[32]

The number of stacked layers or PDMS strips, as well as the adjacent spacing and orientation, could be adjusted due to the bottom-up nature of macroscopic supramolecular assembly. For example, Figure 1b,c shows that a periodically stacked 3D structure was formed with three layers of PDMS strips perpendicular to each other and that the top layer nearly overlapped with the bottom layer, as indicated by the 3D side view. This phenomenon indicates that fabricating 3D ordered structures by combining localization via a magnetic field and immobilization via supramolecular interactions can achieve microscale accuracy in the 3D positioning of the building blocks. The orientation of the PDMS strips could also be adjusted from right angles between the first and second layer to an angle of 60° between

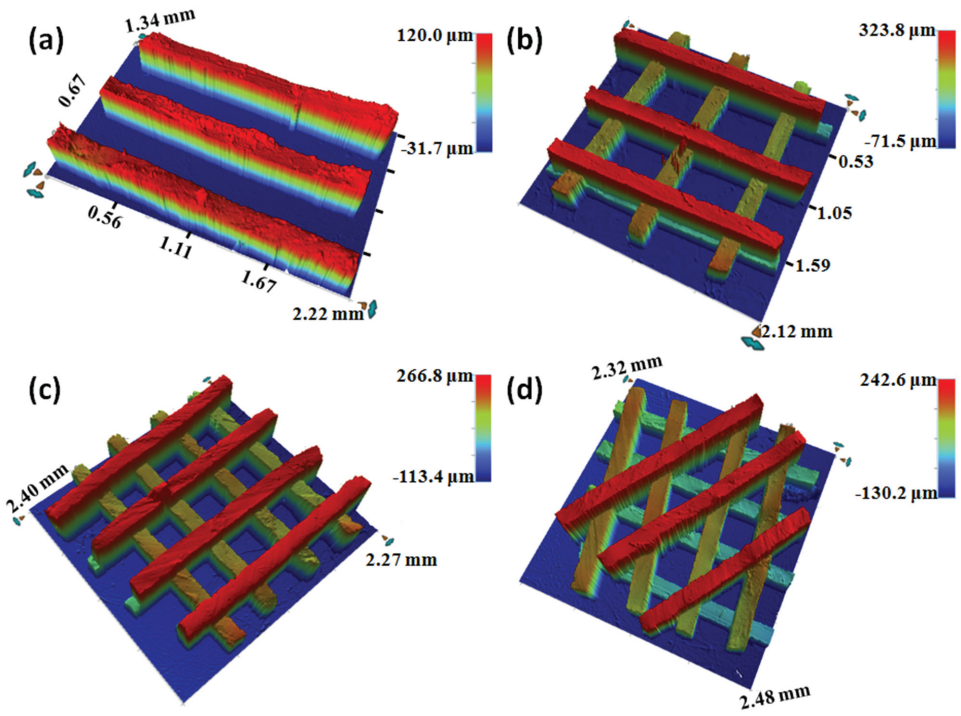

Figure 1. 3D profiled images of a) one layer of PDMS strips parallel to each other with equal adjacent spacing, b) three layers of periodically stacked PDMS strips with a perpendicular orientation of the adjacent layers, c) a narrow horizontal spacing between the PDMS strips compared with that in (b), and d) a layer oriented at an angle of approximately 60° to the underlying layer.

the second and third layer, as displayed in the three staggered layers of strips in Figure 1d. Therefore, the method of macroscopic supramolecular assembly assisted by a magnetic field provided a new strategy to fabricate 3D ordered structures with controllable porous morphologies.

2.5. Bioevaluation of the 3D Ordered Structures

Because the 3D ordered structures prepared by macroscopic supramolecular assembly exhibited regular pores, we anticipated that the microscale porous structures might favor cell growth in 3D cell culture and thus function as 3D scaffolds. For possible biological application, we first evaluated the cell viability of PDMS building blocks through a standard 3-(4,5-dimethylthiazol-2yl)-2,5-diphenyl tetrazolium bromide (MTT) assay with the L929 cell line. We have checked four types of samples: 1) the bare PDMS strips dyed green or red, 2) the PDMS strips modified with $(PDDA/PAA\text{-}CD \text{ or } PAA\text{-}Azo)_{25}$, 3) PDMS strips modified with $(PDDA/PAA\text{-}CD \text{ or } PAA\text{-}Azo)_{25}$-RGD, and 4) 3D ordered structures assembled on glass slides. For the first three types, the PDMS strips were placed at the bottom of a 96-well microtiter plate, and then the L929 cells were seeded at a density of 5×10^4 cells per well, followed by incubation for 24 h. Meanwhile, control cells were cultured in similar medium without PDMS. After treating both cells with MTT, the cell viability (%) relative to that of the control cells was calculated using an equation that reflected the cell

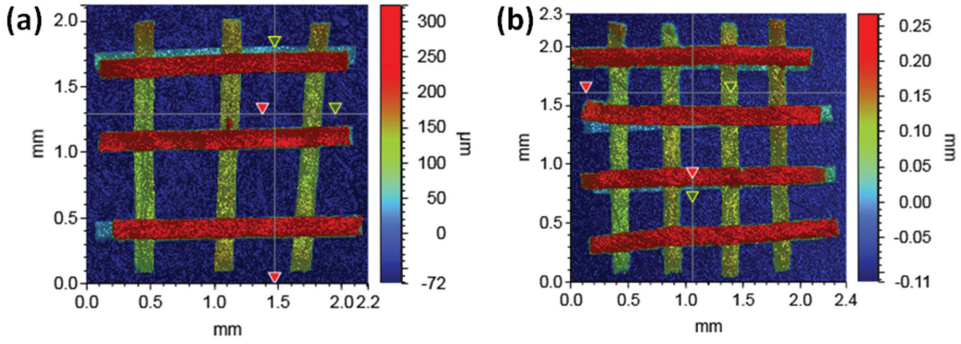

Figure 2. Top view of the as-prepared 3D ordered structures with a) large and b) small adjacent spacing, which corresponds to 3D profile in Figure 2b,c, respectively.

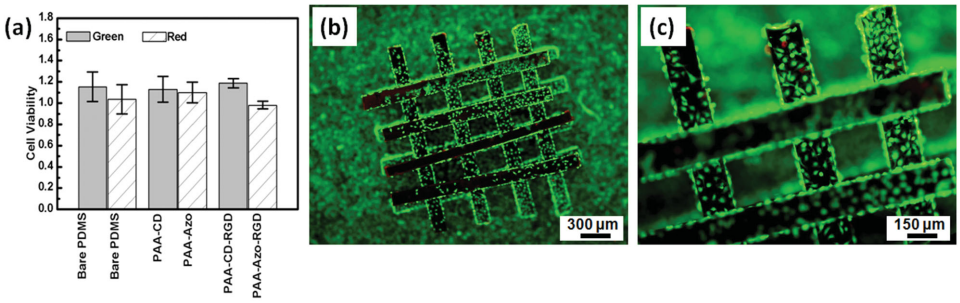

Figure 3. Cell viability was evaluated via a) MTT assay for PDMS building blocks dyed green or red with or without surface modification, and b,c) fluorescence microscopy images of cell adhesion on 3D ordered PDMS structures.

viability ratio, $[A]_{test}/[A]_{control} \times 100\%$, where $[A]_{test}$ and $[A]_{control}$ refer to the absorbance of the tested wells (with PDMS) and control wells (without PDMS), respectively. For comparison, a well-known biocompatible molecule, arginylglycylaspartic acid (RGD), was grafted onto the PDMS surfaces modified with PDDA/PAA-CD or PDDA/PAA-Azo multilayers for identical MTT evaluation. The ratio of cell viability was close to 1.0 for all employed PDMS surfaces (**Figure 3**a), which suggested that the cells remained alive in the presence of PDMS building blocks at a level similar to that of the control experiments. Especially, the cell viability of the PDMS with host or guest groups was comparable to that of the building blocks post-modified with a biocompatible RGD species. This result indicated low toxicity and good cell viability for the involved building blocks and chemicals used in the fabrication of the 3D ordered structures. Besides, the as-prepared 3D ordered structures supported by glass slides were evaluated through a similar procedure with longer culture time in a 12-well microtiter plate by placing the slides at the bottom of the wells. The result in Figure S4 (Supporting Information) showed that the number of the live L929 cells gradually increase with the culture time from 0 to 72 h.

After demonstrating that the applied PDMS materials were non-toxic to cell growth, we further explored the potential application of the 3D ordered structures as scaffolds via cell adsorption experiments with adult stem cells (ASCs), human umbilical vein endothelial cells (HUVECs), and human dermal fibroblast (HDF) cells. Single-cell suspensions of 1×10^5 cells mL^{-1} in media were added to the 3D ordered structures, which were modified with a multilayer of polylysine and poly(aspartic acid) to increase biocompatibility. The polyanion of polylysine is widely used as a biocompatible synthetic amino acid to enhance cell attachment[4,33] and the polycation of poly(aspartic acid) is known with good biodegradability.[34–36] After 3 d, a live/dead assay was performed to determine the number of live (green) or dead (red) cells as observed by fluorescence imaging. As shown in Figure 3b, numerous HUVECs were adsorbed onto the 3D ordered structure, most of which were attached to the building blocks (green). From the local magnification in Figure 3c, the cell morphology demonstrated easy adhesion onto the 3D ordered structures. Similar results were also obtained for the studies using ASCs and HDF cells, as shown in Figure S6 (Supporting Information). These results showed that the 3D ordered structures were suitable as supporting material for cell adhesion and growth and might further work as scaffolds for cell differentiation, which could be meaningful for tissue engineering. Although the cells were also observed to spread on the substrate due to similar treatment with biocompatible coating, it is possible to obtain a freestanding 3D ordered structure by peeling it off the substrate with competitive guest molecules such as adamantane and then use the structure for cell culture in the future.

2.6. Controlled Localization of Targeted Bioactive Species within the Scaffold

Many researchers have recently noted that introducing multi-specific growth factors to precise locations has been a substantial challenge for the fabrication of complex 3D tissue scaffolds.[11,13,37] This is mainly because keeping bioactivity of growth factors during targeted chemical modification in 3D space is difficult. For example, some available methods or techniques, such as 3D printing, involve harsh experimental conditions that are unfavorable to maintaining bioactivity.[5,13] In this research, the proposed strategy of combining magnetic localization with supramolecular assembly provided a proof-of-concept solution to the above challenges. As mentioned, the PDMS materials together with the modification species on the surface have been proven biocompatible. Additionally, supramolecular assembly is a mild and biocompatible bottom-up method that could be used to introduce targeted building blocks with necessary growth factors to designated locations within a 3D ordered structure. To demonstrate this proof-of-concept idea, we fabricated a third PDMS building block type by modifying with PAH-biotin as the polycation and PAA-CD as the polyanion. These provided not only molecular recognition groups for supramolecular assembly but also bioactive sites for subsequent loading of avidin-labeled growth factors. To distinguish between the normally modified PDMS building blocks with CD groups (red) and the Azo groups (green), we labeled the third type of PDMS strips with blue or yellow. As seen in **Figure 4**a,b, during the step-by-step fabrication process, the third type of PDMS building blocks with specific bioactive sites (blue or yellow) was aligned in the second or third row of the second layer; other PDMS building blocks in the same layer were labeled with red. Besides, we have demonstrated that the two molecular recognition systems of CD/Azo and biotin/avidin did not affect each other when they were both present (Figure S7, Supporting Information). This result demonstrated that the building blocks modified with specific bioactive sites

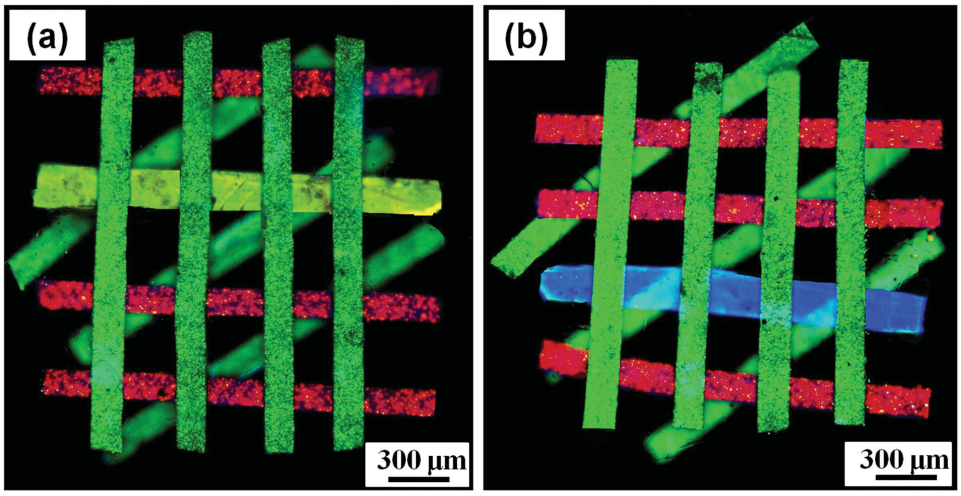

Figure 4. Fluorescent images of the 3D ordered structures with specific bioactive PDMS building blocks in the a) second or b) third row of the second layer.

could be guided to and assembled at designated locations in the 3D ordered structures, which could not be easily achieved by harsh methods such as lithography and 3D printing. Therefore, we believe that by further introducing growth factors through the biorecognition between biotin/avidin groups, macroscopic supramolecular assembly could be used to fabricate 3D ordered structures as scaffolds with targeted modification. Moreover, this proposed strategy is advantageous with flexibility in fabrication of building blocks and inducing supramolecular interactions, thus making it versatile for a wide range of biocompatible materials; the typical material of hydrogel is also suitable in this method (Figure S8, Supporting Information).

3. Conclusion

In summary, we fabricated periodically stacked 3D ordered structures by combining macroscopic supramolecular assembly with magnetic-field-induced localization, which were shown to be biocompatible. Moreover, specific building blocks modified with bioactive sites could be incorporated to targeted locations within the 3D structures. Thus, we developed a proof-of-concept idea for the fabrication of 3D scaffolds with in situ targeted modification of growth factors, which could be meaningful for inducing cell differentiation in future tissue engineering research. This is the first demonstration of obtaining bulk supramolecular materials through macroscopic supramolecular assembly.

4. Experimental Section

Materials and Instruments: The following chemicals were used as supplied. PDDA (aq., wt 20%, M_W 400 000 g mol^{-1}) from Acros Organics; PDMS (Sylgand 184) from Dow Corning; 1H, 1H, 2H, 2H-perfluoroalkyltriethoxysilane, MTT, and polylysine from Sigma–Aldrich; Dulbecco's modified eagle medium (DMEM), fetal bovine serum (FBS, wt 10%), penicillin, streptomycin, live/dead viability/cytotoxicity kit and trypsin–EDTA from Invitrogen, USA; 96-well microtiter plate from Nunc Co., Wiesbaden, Germany. ASC were isolated from inguinal adipose tissue of 3-week-old male Wistar rats according to the Chinese PLA General Hospital Animal Care and Use Committee guidelines following the principles of animal care. HUVEC and HDF cells were purchased from China Center of Type Culture Collection in Wuhan, China. L929 cell lines were from the American Type Culture Collection, Manassas, USA. PAA-CD and PAA-Azo were synthesized following reported methods.[18] Red, green, blue, and yellow dyes were commercially available. If not specifically noted, other normal reagents were purchased from Sinopharm Chemical Reagent Beijing Co., Ltd.

The PDMS cutting at 150 μm was conducted on a freezing microtome instrument (Leica CM1950) from Leica, Wetzlar, Germany. The 3D profiled images were obtained on a 3D microscope contour GT-X (Tucson, AZ, USA). The absorbance of MTT in DMSO was obtained from a microplate reader (Spectra Plus, Tecan, Zurich, Switzerland). The fluorescence images were taken on a fluorescence microscopy (Olympus BX53, Tokyo, Japan). H NMR spectra were obtained at 400 MHz with a Bruker AV400 NMR spectrometer.

MTT Assay of Different PDMS Materials: L929 cells were cultured in DMEM accompanied by heat-inactivated FBS, penicillin (100 units mL^{-1}), and streptomycin (100 μg mL^{-1}) at 37 °C, with a relative humidity of 95% in the presence of CO_2 (5%). Afterward, the cells were seeded in a 96-well microtiter plate with a cell density of approximately 5×10^4 cells well^{-1} and further cultured in 100 μL DMEM well^{-1} for 24 h. Subsequently, 10 μL sterile-filtered MTT (PBS buffer, 5 mg mL^{-1}) was added to each well, followed by storage for 5 h. The precipitated formazan crystals were redissolved in 100 μL DMSO well^{-1} and were detected using a microplate reader (Spectra Plus, Tecan, Zurich, Switzerland) at 570 nm. For the above procedure, bare dyed PDMS with magnetic nanoparticles, PDMS modified with PDDA/PAA-CD or PDDA/PAA-Azo and subsequently modified with RGD were placed at the bottom of the wells and served as the test group; for comparison, the control experiments were carried out under similar conditions but without PDMS.

Cell Adhesion and In Vitro Analyses: HUVEC were cultured in high-glucose DMEM with FBS, penicillin (100 units mL^{-1}), and streptomycin (100 units mL^{-1}) at 37 °C in 5% CO_2 in a humidified incubator until the cells reached 80% confluence. The cells were then passaged using 0.25% (w/v) trypsin–EDTA. Cells at the fourth passage were used in the following experiments. Single-cell suspensions of 1×10^5 cells mL^{-1} in media were added to the 3D structures and incubated in 5% CO_2 at 37 °C for 3 d. The live/dead assay kit was used according to the manufacturer's instructions. To determine viability, images were obtained using fluorescence microscopy with 494 nm (green, Calcein) and 528 nm (red, EthD-1) excitation filters.

Supporting Information

Supporting Information is available from the Wiley Online Library or from the author.

Acknowledgements

This work was supported by NSFC (21374006; 51422302), the Program of the Co-Construction with Beijing Municipal Commission of Education of China, Open Project of State Key Laboratory of Supramolecular Structure and Materials (SKLSSM201517), Beijing Young Talents Plan (YETP0488), and the 863 Projects of Ministry of Science and Technology of China (2012AA020502). The authors do appreciate Dr. Dengli Qiu from Bruker (Beijing) Scientific Technology Co., Ltd. for his kind technical help in obtaining 3D profile of the 3D ordered structures.

Received: August 11, 2015
Revised: September 8, 2015
Published online: October 15, 2015

[1] B. J. Xie, R. L. Parkhill, W. L. Warren, J. E. Smay, *Adv. Funct. Mater.* **2006**, *16*, 1685.
[2] C. A. DeForest, B. D. Polizzotti, K. S. Anseth, *Nat. Mater.* **2009**, *8*, 659.
[3] J. N. H. Shepherd, S. T. Parker, R. F. Shepherd, M. U. Gillette, J. A. Lewis, R. G. Nuzzo, *Adv. Funct. Mater.* **2011**, *21*, 47.
[4] S. Kim, F. Qiu, S. Kim, A. Ghanbari, C. Moon, L. Zhang, Bradley J. Nelson, H. Choi, *Adv. Mater.* **2013**, *25*, 5863.
[5] H.-J. Lee, S.-H. Ahn, G. H. Kim, *Chem. Mater.* **2012**, *24*, 881.
[6] Y. H. Li, G. Y. Huang, X. H. Zhang, B. Q. Li, Y. M. Chen, T. L. Lu, T. J. Lu, F. Xu, *Adv. Funct. Mater.* **2013**, *23*, 660.
[7] S.-Y. Lin, J. Fleming, D. Hetherington, B. Smith, R. Biswas, K. Ho, M. Sigalas, W. Zubrzycki, S. Kurtz, J. Bur, *Nature* **1998**, *394*, 251.
[8] P. Podsiadlo, A. K. Kaushik, E. M. Arruda, A. M. Waas, B. S. Shim, J. Xu, H. Nandivada, B. G. Pumplin, J. Lahann, A. Ramamoorthy, N. A. Kotov, *Science* **2007**, *318*, 80.
[9] D. H. Gracias, J. Tien, T. L. Breen, C. Hsu, G. M. Whitesides, *Science* **2000**, *289*, 1170.
[10] D. Go, T. E. Kodger, J. Sprakelc, A. J. C. Kuehne, *Soft Matter* **2014**, *10*, 8060.
[11] R. G. Wylie, S. Ahsan, Y. Aizawa, K. L. Maxwell, C. M. Morshead, M. S. Shoichet, *Nat. Mater.* **2011**, *10*, 799.
[12] K. Y. Ma, P. Chirarattananon, S. B. Fuller, R. J. Wood, *Science* **2013**, *340*, 603.
[13] S. V. Murphy, A. Atala, *Nat. Nanotechnol.* **2014**, *32*, 773.
[14] A. Harada, R. Kobayashi, Y. Takashima, A. Hashidzume, H. Yamaguchi, *Nat. Chem.* **2011**, *3*, 34.
[15] H. Yamaguchi, Y. Kobayashi, R. Kobayashi, Y. Takashima, A. Hashidzume, A. Harada, *Nat. Commun.* **2012**, *3*, 603.
[16] H. Qi, M. Ghodousi, Y. Du, C. Grun, H. Bae, P. Yin, A. Khademhosseini, *Nat. Commun.* **2013**, *4*, 2275.
[17] Y. L. Han, Y. S. Yang, S. B. Liu, J. H. Wu, Y. M. Chen, T. J. Lu, F. Xu, *Biofabrication* **2013**, *5*, 035004.
[18] M. J. Cheng, F. Shi, J. S. Li, Z. F. Lin, C. Jiang, M. Xiao, Y. J. Zhang, L. Q. Zhang, W. T. Yang, T. Nishi, *Adv. Mater.* **2014**, *26*, 3009.
[19] C. Ma, T. Li, Q. Zhao, X. Yang, J. Wu, Y. Luo, T. Xie, *Adv. Mater.* **2014**, *26*, 5665.
[20] J. W. Steed, J. L. Atwood, *Supramolecular Chemistry*, Wiley, Hoboken, NJ, USA **2009**.
[21] S. W. Kwok, S. A. Morin, B. Mosadegh, J.-H. So, R. F. Shepherd, R. V. Martinez, B. Smith, F. C. Simeone, A. A. Stokes, G. M. Whitesides, *Adv. Funct. Mater.* **2014**, *24*, 2180.
[22] E. Diller, M. Sitti, *Adv. Funct. Mater.* **2014**, *24*, 4397.
[23] F. Shi, S. H. Liu, H. T. Gao, N. Ding, L. J. Dong, W. Tremel, W. Knoll, *Adv. Mater.* **2009**, *21*, 1927.
[24] M. J. Cheng, H. T. Gao, Y. J. Zhang, W. Tremel, J.-F. Chen, F. Shi, W. Knoll, *Langmuir* **2011**, *27*, 6559.
[25] M. J. Cheng, Q. Liu, Y. M. Xian, F. Shi, *ACS. Appl. Mater. Interfaces* **2014**, *6*, 7572.
[26] a) H. Deng, X. L. Li, Q. Peng, X. Wang, J. P. Chen, Y. D. Li, *Angew. Chem.* **2005**, *117*, 2842; b) H. Deng, X. L. Li, Q. Peng, X. Wang, J. P. Chen, Y. D. Li, *Angew. Chem. Int. Ed.* **2005**, *44*, 2782.
[27] Y. Zhou, D. S. Wang, S. L. Huang, G. Auernhammer, Y. J. He, H.-J. Butta, S. Wu, *Chem. Commun.* **2015**, *51*, 2725.
[28] X. Zhang, *Acta Polym. Sin.* **2007**, *10*, 905.
[29] F. Shi, Z. Liu, G. L. Wu, M. Zhang, H. Chen, Z. Q. Wang, X. Zhang, I. Willner, *Adv. Funct. Mater.* **2007**, *17*, 1821.
[30] M. J. Cheng, C. Jiang, Z. Y. Ding, Y. J. Zhang, Y. Fu, F. Shi, *Phys. Chem. Chem. Phys.* **2013**, *15*, 15172.
[31] C. Jiang, X. L. Liu, C. J. Luo, Y. J. Zhang, L. Shao, F. Shi, *J. Mater. Chem. A* **2014**, *2*, 14048.
[32] D. J. Lipomi, F. Ilievski, B. J. Wiley, P. B. Deotare, M. Lončar, G. M. Whitesides, *ACS Nano* **2009**, *3*, 3315.
[33] S. B. Hartono, W. Gu, F. Kleitz, J. Liu, L. He, A. P. J. Middelberg, C. Yu, G. Q. Lu, S. Z. Qiao, *ACS Nano* **2012**, *6*, 2104.
[34] T. Kakuchi, *Macromolecules* **1998**, *31*, 2107.
[35] J.-J. Nie, X.-B. Dou, H. Hu, B. Yu, D.-F. Chen, R.-X. Wang, F.-J. Xu, *ACS Appl. Mater. Interfaces* **2015**, *7*, 553.
[36] H. Arimura, Y. Ohya, T. Ouchi, *Macromolecules* **1998**, *31*, 2107.
[37] J. Cabanas-Danés, E. D. Rodrigues, E. Landman, J. V. Weerd, C. V. Blitterswijk, T. Verrips, J. Huskens, M. Karperien, P. Jonkheijm, *J. Am. Chem. Soc.* **2014**, *136*, 12675.